frontiers | Frontiers in Marine Science

TYPE Original Research
PUBLISHED 23 August 2022
DOI 10.3389/fmars.2022.975184

OPEN ACCESS

EDITED BY
Yuanyuan Feng,
Shanghai Jiao Tong University, China

REVIEWED BY
Peng Jin,
University of Guangzhou, China
Mark Moore,
University of Southampton,
United Kingdom

*CORRESPONDENCE
Liangliang Kong
liangliang.kong@mail.mcgill.ca

SPECIALTY SECTION
This article was submitted to Global Change and the Future Ocean, a section of the journal Frontiers in Marine Science

RECEIVED 22 June 2022
ACCEPTED 08 August 2022
PUBLISHED 23 August 2022

CITATION
Kong L and Price NM (2022) Long-term adaptive response of an oceanic diatom to copper deficiency. *Front. Mar. Sci.* 9:975184. doi: 10.3389/fmars.2022.975184

Long-term adaptive response of an oceanic diatom to copper deficiency

Liangliang Kong[1,2*] and Neil M. Price[2]

[1]College of Marine Life Sciences, Ocean University of China, Qingdao, China, [2]Department of Biology, McGill University, Montréal, QC, Canada

Enhanced vertical stratification brought about by warming of the ocean surface is expected to reduce vertical circulation and nutrient input with knock-on effects for phytoplankton. Increased nutrient limitation is one predicted outcome, but how that will impact phytoplankton is uncertain because we do not know how they will adapt. We used copper (Cu) as a model catalytic nutrient to explore the adaptive response of an oceanic diatom to continuous nutrient deprivation in laboratory experiments. Populations of *Thalassiosira oceanica* maintained under Cu-limiting and sufficient conditions for ~380 generations differed significantly in their abilities to grow in medium containing 1 nM Cu. Continued selection for more than 2000 generations increased Cu use efficiency (CuUE) of a low Cu-adapted (LCuA) population by more than 2-fold compared to the control and ancestral populations. The increase in CuUE resulted from a decrease in the amount of cellular Cu required for growth and an increase in the net carbon assimilation rate. Redistribution of cellular Cu and increased efficiency of photosynthetic reactions are hypothesized to explain the fast rates of maximum electron transport of low Cu-adapted cells despite containing less Cu. The results show that adaptation increased resource use efficiency in phytoplankton, which could reduce the impact of increased nutrient deficiency in the future ocean.

KEYWORDS

adaptive response, copper deficiency, copper use efficiency, diatom, long-term adaptation

Introduction

Copper quotas (Q_{Cu}) of phytoplankton are maintained within narrow limits by cellular regulatory processes even as environmental concentrations vary by orders of magnitude (Sunda and Huntsman, 1995; Page et al., 2009). The quotas are set by the amounts of Cu-redox proteins required in cellular metabolism (Merchant et al., 2006; Kim and Price, 2017; Kong and Price, 2022) and depend upon uptake of Cu from the environment. Decreased Cu bioavailability can cause Q_{Cu} to decline and become limiting

for Cu-dependent metabolism and growth, whereas at high concentrations cellular Cu may accumulate to toxic levels (Sunda and Guillard, 1976; Brand et al., 1986; Kong and Price, 2019). For most of the ocean, however, dissolved Cu is in the nanomolar range (avg. ~1 nM), and like other essential trace metal nutrients, predominantly complexed by organic ligands (>99%) (Moffett and Dupont, 2007; Jacquot et al., 2013; Jacquot and Moffett, 2015; Whitby et al., 2018). Under these conditions, low Cu concentration can limit phytoplankton biomass and reduce Fe uptake by large species (Peers et al., 2005; Takeda et al., 2014; Semeniuk et al., 2015), so that changes in Cu bioavailability could influence production in some ocean ecosystems.

Environmental change has had a strong effect on ocean physics and chemistry, warming the surface layers and lowering the pH (Houghton et al., 2001; Caldeira and Wickett, 2003). Lower pH brought about by increased atmospheric CO_2, reduces the concentration of hydroxide and carbonate ions (Orr, 2011), with significant consequences for trace metal speciation (Millero et al., 2009). Equilibrium concentrations of hydrated Cu^{2+} and inorganic Cu(II) species are estimated to increase by ca. 5-fold as pH declines to 7.4 due to a decrease in $CuCO_3$ and Cu-complexation by organic ligands (Millero et al., 2009; Gledhill et al., 2015; Avendaño et al., 2016). Ocean warming, on the other hand, enhances upper ocean stratification and weakens ocean circulation (Sarmiento et al., 1998), making the resupply of limiting resources from deep waters more difficult. Time series analysis already shows a decrease in nutrient concentration in some regions (Taylor et al., 2012), consistent with predictions. Increased stratification in oligotrophic gyres is affecting nutrient supply from deep waters and phytoplankton production in the surface (Behrenfeld et al., 2006). In addition, some modeling results indicate global warming could alter supply of aeolian dust (Zhang et al., 2020; Zong et al., 2021), an important source of nutrients to ocean systems and occasionally having negative effects on phytoplankton due to toxicity of Cu-rich aerosol input (Paytan et al., 2009; Jordi et al., 2012). Changes in resource availability are thus expected in the future ocean and may exert a significant impact on productivity and biogeochemical cycles (Joos et al., 1999; Boyd and Doney, 2002; Behrenfeld et al., 2006). The impact on phytoplankton, however, will be modulated by phenotypic plasticity and by adaptation, resulting in uncertain outcomes (Litchman et al., 2012; Merilä and Hendry, 2014). Predicting phytoplankton responses requires understanding how adaptation proceeds, because changes in the environment will occur over time scales longer than the life span of individuals.

Much attention has been given to short-term acclimation of phytoplankton to changes in resource availability. Increased elemental acquisition and intracellular mobilization of stored resources are the most immediate responses to nutrient limitation, which buffer the decline in ambient nutrient availability but may be ineffective to relieve the deficiency at extremely low environmental levels (Morel, 1987; Merchant and Helmann, 2012). The primary outcome is depletion of intracellular nutrient stores. In some organisms, acclimation strategies include conditional expression of alternative enzymes or pathways with different resource dependencies (LaRoche et al., 1996; Castruita et al., 2011). For example, a Cu-sparing pathway in green algae replaces Cu-containing plastocyanin with an Fe-containing cytochrome c_6 in response to Cu limitation (Merchant and Bogorad, 1986a). Short-term acclimation induces conditional expression of alternative pathways without changing the genotypes and allows a temporal adjustment of intracellular elemental stoichiometry to cope with nutrient deficiency (Strzepek and Price, 2000; Geider and LaRoche, 2002; Bertilsson et al., 2003), but it may give little insight into the long-term evolutionary response that is normally caused by genotypic variations under selection pressure.

Adaptive evolution produces novel solutions for organisms to survive in new environments, leading to improved phenotypes with higher fitness. Selection for low metal tolerance is thought to be the reason that oceanic phytoplankton require less Fe, Mn and Zn to sustain maximum growth than coastal species, which inhabit metal-rich environments (Brand et al., 1983; Sunda et al., 1991; Strzepek and Harrison, 2004; Strzepek et al., 2012). The decreased metal demand of the oceanic strains is hypothesized to be an adaptive response to nutrient limitation (Brand et al., 1983), but the hypothesis is based mainly on a *post-hoc* rationalization without experimental support. Experimental evolution driven by natural selection provides an effective way to study adaptive response of phytoplankton to changes in the environment. So far, studies on phytoplankton adaptation are limited to temperature and CO_2, which are projected to increase substantially in the future (Collins and Bell, 2004; Lohbeck et al., 2012; Jin et al., 2013; Schlüter et al., 2014; Hutchins et al., 2015; Schlüter et al., 2016; O'Donnell et al., 2018; Schaum et al., 2018; Tong et al., 2018; Jin et al., 2022). Evolution under elevated CO_2 concentration, however, has little bearing on adaptive responses to nutrient limitation, which is pervasive in the open sea (Mills et al., 2004; Moore et al., 2013; Browning et al., 2017). Adaptation of phytoplankton to nutrient limitation is rarely tested experimentally. McDonnell (2015) examined the response of a green alga, *Chlamydomonas* sp., to phosphorus deficiency and observed that the evolved populations contained less limiting resource per unit cell volume than the ancestral population.

Here we report our findings on the adaptive responses of *T. oceanica* after more than 2000 generations under Cu-limiting and sufficient conditions. Adapted populations were assessed for growth rate, photosynthetic performance, elemental stoichiometry, and transcript abundance of key Cu-containing proteins. The results show that the low Cu-adapted population required less cellular Cu and sustained faster rates of growth under Cu-limiting conditions than the ancestral and control populations.

Materials and methods

Thalassiosira oceanica CCMP1005 was obtained from the National Center for Marine Algae and Microbiota (NCMA) at Bigelow Laboratory (https://www.bigelow.org/) from a cryopreserved stock originally prepared in 2007. Prior to cryopreservation, the culture was maintained in natural seawater medium enriched with f/2 nutrients (Guillard and Ryther, 1962) and transferred every two weeks. The culture was subsequently transferred into artificial seawater medium, Aquil (Price et al., 1989), in our laboratory and grown under Cu-sufficient conditions (21.4 nM Cu) in 28 mL polycarbonate tubes at 20°C with continuous illumination of 200 µmol photons m^{-2} s^{-1} (Kong and Price, 2019). Prior to the evolutionary selection experiment, *T. oceanica* was cultivated in the NCMA and our laboratory for dozens of years so it presumably represented a population with a large variety of pre-existing genotypes, rather than a single clone.

The selection experiment was initiated by inoculating a small volume of the Cu-sufficient population (~2×10^5 cells) into Cu-deficient medium containing 2.5 nM or 1 nM Cu. Cells grew at the maximum rate in Cu-sufficient medium with 21.4 nM Cu, but were growth limited by Cu in the Cu-deficient media (Kong and Price, 2019). The same *T. oceanica* population was cultivated simultaneously in Cu-sufficient medium and used as a control for evaluating potential artifacts created by our laboratory environment and the culturing method. Two replicate cultures of the three selection lines (1, 2.5 and 21.4 nM Cu) were cultivated in low density, batch cultures in 28 mL polycarbonate tubes under identical growth conditions. In this culturing technique, a subsample of the exponentially growing population was transferred into fresh medium, grown until late exponential phase, and then transferred again into fresh medium. The initial cell density in each batch culture was *ca.* 8000-10000 cells ml^{-1}, so that ~2 to 3×10^5 cells were transferred each time into fresh medium. Less than 20% of copper added to the media was consumed by the time the populations were in late exponential phase. All other nutrient resources in the media were provided in excess. Thus, the nutrient chemistry of the cultures was kept relatively constant. Specific growth rate was calculated for each batch culture from linear regression analysis of ln(*in vivo* chlorophyll fluorescence) as a function of elapsed time.

The initial selection experiment continued for ~1 year at which time the populations were evaluated for differences in growth in Cu-limiting medium. From then on, only a single replicate of each of the three selection lines was maintained for another 3.5 years, corresponding to approximately 2300 generations of reproduction in the Cu-deficient medium and 3600 generations in the Cu-sufficient medium. The number of generations (#gen) was estimated by the formula: #gen = t/(ln2/µ′), where t is elapsed time (day) and µ′ is the normalized specific growth rate (µ) for each batch culture. The normalized µ′ was calculated by the linear regression formula reported in Table 2. The total number of generations was the sum of number of generations for each batch culture. The evolved populations in Cu-deficient medium (1 and 2.5 nM Cu) were designated as low Cu-adapted ($LCuA_{1nM}$ and $LCuA_{2.5nM}$) and the populations selected in Cu-sufficient medium (21.4 nM Cu) designated as the control Cu-adapted (CCuA) populations. To compare physiological traits of the adapted populations with their ancestral phenotype, a fresh culture of *T. oceanica* 1005 was obtained from the NCMA and used as an ancestral population to represent the Cu nutritional phenotype of the diatom before the selection experiment. Once the fresh cryopreserved culture arrived in our laboratory, it was transferred to Cu-sufficient medium and grown as described above. The ancestral population thus experienced identical growth conditions as the CCuA population, but only for about 100 generations before it was sampled for physiological traits.

A reciprocal transplant assay was conducted at the end of the selection experiment to investigate whether long-term adaptation changed cell physiology and elemental stoichiometry. All samples were obtained from cultures harvested in mid-exponential phase of growth. Assays for each population ($LCuA_{1nM}$, CCuA and ancestral) were conducted in Cu-sufficient and deficient medium. Prior to the assays, the CCuA and ancestral populations were acclimated in Cu-deficient medium (1 nM Cu) for 30-50 generations and the $LCuA_{1nM}$ population was acclimated in Cu-sufficient medium (21.4 nM Cu) for 30-50 generations. Specific growth rates of replicate cultures were calculated as described above. Cell volume and surface area were determined from linear dimensions of 20 randomly selected cells using a light microscope, assuming a cylindrical cell shape (Hillebrand et al., 1999). Cellular chlorophyll *a* was measured spectrophotometrically (Kong and Price, 2020). Chlorophyll fluorescence-derived photosynthetic parameters (Ralph and Gademann, 2005), maximum quantum yield of photosystem II (F_v/F_m), effective quantum yield of photosystem II (Φ_{PSII}) and maximum relative electron transport rate ($rETR_{max}$), were measured using a Water-PAM Fluorometer (Heinz Walz GmbH, Effeltrich, Germany) according to Kim and Price (2017). Cellular Cu and particulate carbon were measured by graphite furnace atomic absorbance spectrophotometry (Kim and Price, 2017) and with ^{14}C-labelled sodium bicarbonate ($NaH^{14}CO_3$, 48.7 mCi $mmol^{-1}$, New England Nuclear; McDonnell, 2015), respectively. Difference among traits were tested by one-way ANOVA and Tukey's *post hoc* comparisons performed in R 4.0.3 (R Core Team, 2020). The interaction between selection regime and assay condition on growth rate in the reciprocal assay was tested by a linear mixed-effects model (Jin et al., 2022). The effect of selection time on growth rate of

the populations was evaluated by ANCOVA (analysis of covariance) in R.

Transcript abundance of key Cu-containing proteins was quantified in Cu-limited CCuA and $LCuA_{1nM}$ cells by an mRNA sequencing (RNAseq) project (Kong et al., unpublished). CCuA and $LCuA_{1nM}$ cells were acclimated in Cu-deficient medium and harvested in mid-exponential growth phase onto 1 µm polycarbonate filters. Total RNA was purified from ~70 million cells using a Plant RNA Purification Kit with an on-column TURBO DNase digestion step (Thermo Fisher Scientific, ON, Canada). Messenger RNA was isolated from 1 µg total RNA and cDNA sequencing libraries were constructed with fragmented mRNA by a TruSeq™ RNA Sample Preparation Kit (Illumina, CA, USA), as per the manufacturer's recommendation. Paired-end libraries were quantified and submitted to an Illumina Paired-end 150 bp sequencing lane on an Illumina HiSeq 3000 Sequencing System. Sequencing library preparation and mRNA sequencing were performed by Shanghai Biozeron Biotechnology Co., Ltd (Shanghai, China). Raw RNAseq reads were processed and used for *de novo* transcriptome assembly according to Kong and Price (2022). Key Cu-containing proteins in assembled transcriptomes were identified by BLAST search using known Cu-containing protein sequences. Transcript abundance was calculated by RSEM (RNA-Seq by Expectation Maximization) and expressed as RPKM (Reads Per Kilobase of exon per Million reads mapped) values (Kong and Price, 2022).

Results

Temporal change in growth rate

No change in specific growth rate was observed in the CCuA populations over the first ~340 days of the experiment, but a significant positive increase occurred in the LCuA populations that was inversely related to Cu concentration (Figure 1). Regression analysis showed the replicates had similar slopes and intercepts (Table 1). We evaluated the effect of selection on the growth rates of the CCuA and $LCuA_{1nM}$ populations in a common garden experiment in 1 nM Cu-deficient medium. The CCuA population was grown first in the low Cu medium for 20 generations to allow for physiological acclimation. Results of the experiment revealed significant differences between the low and high Cu adapted lines ($p<0.05$, ANOVA) (Figure 1). The $LCuA_{1nM}$ populations grew about 23-37% faster than the CCuA populations in low Cu medium, consistent with the observed increase in specific growth rate during the initial adaptation.

Continued selection of a CCuA population for an additional 3.5 years in Cu-replete medium caused a significant increase in growth rate from ~1.40 to 1.60 d^{-1} ($F_{(1,421)} = 94.8$, $p<0.0001$, ANOVA; Figure 2) despite no observable changes initially. The time series of growth rate fitted by a linear plateau model indicated the population growth rate stabilized at 1.60 d^{-1} after 973 days of selection (Table 2; Supplementary Figure S1).

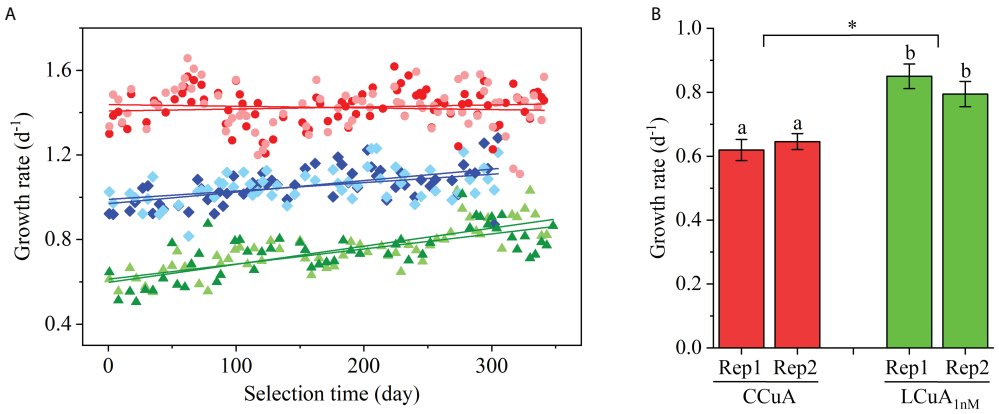

FIGURE 1
(A) Specific growth rate (d^{-1}) of *T. oceanica* as a function of selection time in Cu-sufficient (●) and Cu-deficient media containing 2.5 nM (◆) or 1 nM (▲) Cu. Replicate cultures (n = 2) of the treatments are distinguished by color shades. Each data point represents the specific growth rate of one batch culture. Solid lines are the least squares linear regressions of growth rate as a function of selection time for each population. **(B)** Specific growth rate (d^{-1}) of $LCuA_{1nM}$ and CCuA cells grown in Cu-deficient medium containing 1 nM Cu. $LCuA_{1nM}$ and CCuA cells were harvested after approximately 340 days of adaptation in Cu-deficient and Cu-sufficient medium. CCuA cells were acclimated in Cu-deficient medium for more than 20 generations before measuring growth rate in Cu-deficient medium. Different lowercase letters indicate a significant difference between cultures ($p<0.05$, ANOVA) and an asterisk indicates a significant difference between CCuA and $LCuA_{1nM}$ cells ($p<0.05$, ANOVA).

TABLE 1 Linear regression statistics of growth rate (d^{-1}) of low Cu-adapted ($LCuA_{1nM}$ and $LCuA_{2.5nM}$) and control (CCuA) populations as a function of selection time for the initial selection experiment.

Population	Selection time (d)	Slope (d^{-1}/d) ($\times 10^{-4}$)	Intercept (d^{-1})	Pearson's r	F-statistic	*p*
CCuA-rep1 (●)	341	0.96 ± 0.93^{a}	1.41 ± 0.02^{a}	0.115	$F_{(1,81)} = 1.09$	0.30
CCuA-rep2 (●)	341	-0.78 ± 0.94^{a}	1.44 ± 0.02^{a}	-0.078	$F_{(1,77)} = 0.475$	0.49
$LCuA_{2.5nM}$-rep1 (◆)	305	5.44 ± 1.06^{bc}	0.97 ± 0.02^{b}	0.566	$F_{(1,56)} = 26.37$	<0.001
$LCuA_{2.5nM}$-rep2 (◆)	305	3.97 ± 1.04^{b}	0.99 ± 0.02^{b}	0.455	$F_{(1,56)} = 14.65$	<0.001
$LCuA_{1nM}$-rep1 (▲)	348	8.55 ± 0.82^{c}	0.60 ± 0.02^{c}	0.804	$F_{(1,59)} = 108.21$	<0.001
$LCuA_{1nM}$-rep2 (▲)	348	7.14 ± 1.02^{c}	0.61 ± 0.02^{c}	0.698	$F_{(1,51)} = 48.42$	<0.001

The regression slopes and intercepts are means ± standard error. Different lowercase letters indicate a significant difference ($p<0.05$, ANCOVA). Color dots beside population names correspond to symbols in Figure 1.

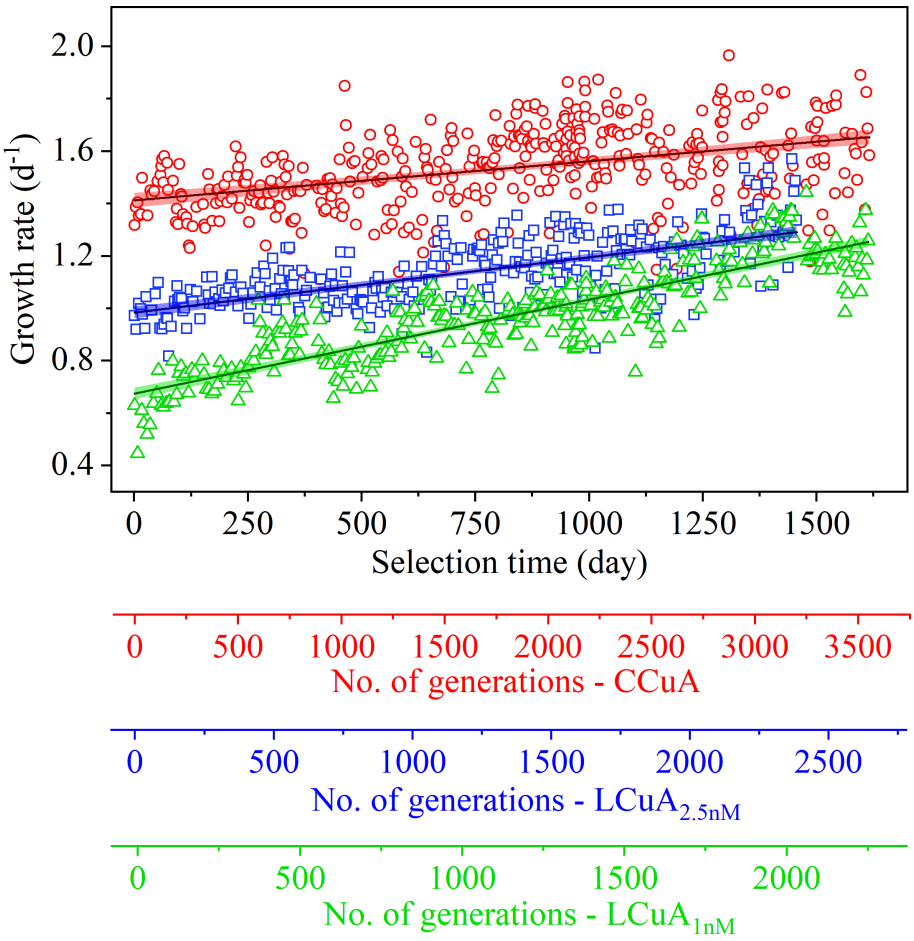

FIGURE 2
Specific growth rate (d^{-1}) of *T. oceanica* as a function of selection time in Cu-sufficient (○) and Cu-deficient medium containing 2.5 nM (□) or 1 nM (△) Cu. The number of cell generations corresponding to the selection time is reported for the control (CCuA) and low Cu-adapted ($LCuA_{2.5nM}$, $LCuA_{1nM}$) populations. Each data point represents the specific growth rate of one batch culture. Solid lines are the least squares linear regressions of growth rate as a function of selection time for each population. Color bands surrounding the regression lines represent the 95% confidence interval.

Growth rates of the $LCuA_{1nM}$ and $LCuA_{2.5nM}$ populations increased continuously, from ~0.60 to 1.20 d^{-1} ($F_{(1,340)}$ = 948.9, p<0.0001) and from ~0.98 to 1.33 d^{-1} ($F_{(1,290)}$ = 308.7, p<0.0001), respectively, over the same time period (Figure 2, Table 2). The rate of change of growth rate was much faster in the LCuA than the CCuA populations and increased with declining Cu concentrations in the growth media (slopes of growth rate versus selection time: 3.59×10^{-4}, 2.21×10^{-4} and 1.49×10^{-4} d^{-1}/d for the $LCuA_{1nM}$, $LCuA_{2.5nM}$ and $CCuA_{21.4nM}$ populations, respectively, p<0.0001, ANCOVA; Table 2). At the end of the selection experiment, growth rates of the LCuA populations were ~80% of the maximum (0.8 μ_{max}) and showed no signs of slowing (Supplementary Figure S2).

Physiological traits

Physiological traits of the long-term $LCuA_{1nM}$ population were measured and compared to CCuA and ancestral populations to assess adaptive responses to Cu deficiency. Growth rates of all populations were significantly slower in Cu-deficient than in Cu-sufficient medium (p<0.001, ANOVA) (Figure 3). The $LCuA_{1nM}$ population grew significantly faster than the CCuA population in Cu-deficient medium (1.19 d^{-1} vs 0.81 d^{-1}), but significantly slower in Cu-sufficient medium (1.37 d^{-1} vs 1.63 d^{-1}) (Figure 3A). The ancestral population had the slowest growth under both conditions (Figure 3A). Growth rate analyzed by a linear mixed-effects model identified a significant interaction between selection regime (Cu-sufficient and Cu-deficient) and assay condition (Cu-sufficient and Cu-deficient) ($F_{1,24}$ = 149.1, p<0.0001; Supplementary Table S1), demonstrating specific adaptation of the $LCuA_{1nM}$ population to Cu deficiency. Copper concentration in the assay environment had no effect on cell size, but long-term adaption decreased the size of $LCuA_{1nM}$ compared to CCuA cells by 15% (p<0.05) (Figure 3B). Cells in the ancestral population were significantly smaller than in both adapted populations. Cellular chlorophyll *a* content was not significantly affected by Cu level in the bioassays. $LCuA_{1nM}$ cells contained between 54 and 71% less chlorophyll *a* L^{-1}-CV (per liter cell volume) than cells in the other populations (Figure 3C).

Active fluorescence measurements showed maximum quantum yield of photosystem II (F_v/F_m) was not significantly affected by Cu availability (Figure 3D). In Cu-deficient medium, all populations had lower effective quantum yield (Φ_{PSII}) compared to Cu-sufficient conditions (p<0.05, Figure 3E). Long-term adaptation increased Φ_{PSII} of the $LCuA_{1nM}$ cells in Cu-deficient medium compared to CCuA and ancestral cells by 19% and 27% (p<0.05), respectively. The maximum relative electron transport rate ($rETR_{max}$) decreased by 32% (p<0.001) in CCuA cells and by 28% (p<0.001) in ancestral cells in response to short-term Cu deficiency, while $rETR_{max}$ of $LCuA_{1nM}$ cells was not significantly affected (Figure 3F). Under Cu limiting conditions, $rETR_{max}$ of $LCuA_{1nM}$ cells was 33% and 57% faster than in CCuA and ancestral cells (p<0.001), respectively.

Copper/Carbon stoichiometry

The cellular Cu quota of $LCuA_{1nM}$ cells (0.20 amol Cu $cell^{-1}$ or 2.15 µmol Cu L^{-1}-CV) was significantly lower than CCuA cells (p<0.05) under Cu-limiting conditions (Table 3). Long-term selection decreased the volumetric carbon quotas in the adapted populations equally (Table 3), so the Cu to C ratio (Cu:C) of the $LCuA_{1nM}$ population was about 32% lower than the CCuA. The ancestral population contained higher volumetric Cu and C quotas under the low Cu assay conditions, but similar cellular Cu:C ratios as the CCuA population (p>0.05) (Table 3). Copper use efficiency (CuUE), computed from Q_{Cu} and C quota (Q_C) and specific growth rate (µ) as CuUE (Q_C/Q_{Cu}) = × µ, was 2.2 to 3.1-fold

TABLE 2 Linear regression statistics of growth rate (d^{-1}) of the low Cu-adapted ($LCuA_{1nM}$, $LCuA_{2.5nM}$) and control (CCuA) populations as a function of selection time for the entire selection experiment.

Population	Selection time (d)	Slope (d^{-1}/d)(×10^{-4})	Intercept (d^{-1})	Pearson's r	F-statistic	*p*
$LCuA_{1nM}$	1-973	3.44 ± 0.29^{a}	0.68 ± 0.02^{a}	0.74	$F_{(1,195)}$ = 242.2	<0.0001
$LCuA_{1nM}$	973-1614	4.55 ± 0.43^{b}	0.55 ± 0.06^{b}	0.66	$F_{(1,143)}$ = 113.7	<0.0001
$LCuA_{1nM}$	1-1614	3.59 ± 0.12^{a}	0.67 ± 0.01^{a}	0.86	$F_{(1,340)}$ = 948.9	<0.0001
$LCuA_{2.5nM}$	1-973	2.15 ± 0.28^{c}	0.98 ± 0.02^{c}	0.60	$F_{(1,208)}$ = 116.2	<0.0001
$LCuA_{2.5nM}$	973-1457	3.08 ± 0.89^{abc}	0.88 ± 0.10^{c}	0.46	$F_{(1,80)}$ = 21.25	<0.0001
$LCuA_{2.5nM}$	1-1457	2.21 ± 0.16^{c}	0.98 ± 0.01^{c}	0.72	$F_{(1,290)}$ = 308.7	<0.0001
CCuA	1-973	2.34 ± 0.25^{c}	1.37 ± 0.02^{d}	0.50	$F_{(1,259)}$ = 87.1	<0.0001
CCuA	973-1616	-0.49 ± 0.41^{d}	1.65 ± 0.05^{e}	-0.06	$F_{(1,160)}$ = 0.60	0.439
CCuA	1-1616	1.49 ± 0.12^{e}	1.41 ± 0.01^{f}	0.43	$F_{(1,421)}$ = 94.8	<0.0001

The regression slopes and intercepts are means ± standard error. Different lowercase letters indicate a significant difference (p<0.05, ANCOVA).

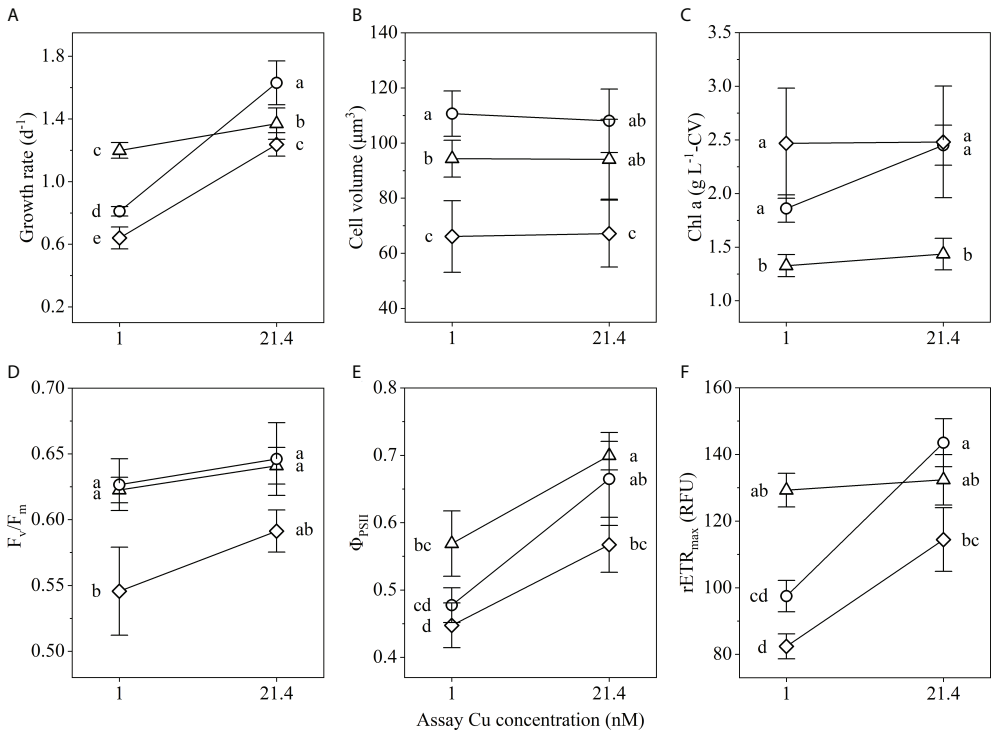

FIGURE 3
Physiological traits of $LCuA_{1nM}$ (△), CCuA (○) and ancestral (◇) populations in Cu-deficient and Cu-sufficient medium: **(A)** specific growth rate, **(B)** cell volume, **(C)** cell volume-normalized chlorophyll *a*, **(D)** maximum quantum yield of photosystem II (F_v/F_m), **(E)** effective quantum yield of photosystem II (Φ_{PSII}) and **(F)** maximum relative electron transport rate ($rETR_{max}$). Error bars represent ±1 SD of three to fifteen biological replicates (n=10-15 for A and B; n=3 for C-F). Different lowercase letters indicate a significant difference among traits of the populations ($p<0.05$, one-way ANOVA).

higher in the $LCuA_{1nM}$ population than in the CCuA and ancestral lines. Thus, $LCuA_{1nM}$ cells had faster rates of carbon fixation per unit of Cu. In absolute terms, the net rate of C assimilation of the $LCuA_{1nM}$ population (0.90 pmol C $cell^{-1}$ d^{-1}) was about 30% faster than in the CCuA population (0.70 pmol C $cell^{-1}$ d^{-1}). Steady-state Cu uptake rates were similar in the adapted and ancestral lines (Table 3).

Expression level of Cu-containing proteins

Expression levels of genes encoding known Cu-containing proteins were quantified by a whole-cell transcriptome analysis of the $LCuA_{1nM}$ and CCuA populations acclimated in Cu-deficient medium (Kong et al., unpublished). Plastocyanin

TABLE 3 Physiological traits and elemental composition of $LCuA_{1nM}$, CCuA and ancestral populations in Cu-deficient medium.

Population	Growth rate (d^{-1})	Cell volume (μm^3)	Cell SA (μm^2)	Q_{Cu} (amol $cell^{-1}$)	Q_{Cu} (μmol L^{-1}-CV)	Q_C (mol L^{-1}-CV)	Cu:C (μmol Cu mol^{-1} C)	CuUE (mol C μmol^{-1} Cu d^{-1})	ρ^{ss} (amol Cu $cell^{-1}$ d^{-1})
$LCuA_{1nM}$	1.20 ± 0.05^a	94.3 ± 6.7^a	119.3 ± 7.0^a	0.20 ± 0.02^a	2.15 ± 0.18^a	8.00 ± 0.29^a	0.27 ± 0.02^a	4.45 ± 0.45^a	0.24 ± 0.02^a
CCuA	0.81 ± 0.03^b	110.7 ± 8.2^b	129.4 ± 7.9^a	0.34 ± 0.06^b	3.10 ± 0.53^b	7.75 ± 0.22^a	0.40 ± 0.07^a	2.03 ± 0.36^b	0.28 ± 0.05^a
Ancestral	0.63 ± 0.07^c	66.1 ± 13.0^c	100.8 ± 12.0^b	0.38 ± 0.09^b	5.71 ± 1.31^c	12.80 ± 0.72^b	0.45 ± 0.11^a	1.41 ± 0.37^b	0.24 ± 0.06^a

Values reported are means ±1 SD of ten to fifteen biological replicates of growth rate and three independent biological replicates of cell volume-normalized carbon (Q_C) and Cu (Q_{Cu}) quota. Copper to carbon ratio (Cu:C), Cu use efficiency (CuUE) and steady-state Cu uptake rate (ρ^{ss}) were calculated using the means of growth rate, Q_C and Q_{Cu} with error propagation. Different lowercase letters indicate a significant difference among physiological traits of the populations ($p<0.05$, ANOVA).

transcript abundance increased by 1.8-fold ($p<0.01$, t-test) in $LCuA_{1nM}$ relative to CCuA cells (Table 4). Transcripts of genes of other Cu-containing proteins decreased ($p<0.05$) or were not significantly affected by selection ($p>0.05$, Table 4). The downregulated genes of tyrosinase, NADH dehydrogenase, NADH:ubiquinone oxidoreductase and cytochrome *c* oxidase 6b decreased by ~1.5 to 30-fold.

Discussion

The experiments described here examined how an oceanic diatom adapted to persistent Cu deficiency, the first such investigation of phytoplankton adaptation to resource deficiency. Adaptation to low Cu significantly increased the growth rate of *T. oceanica* in 1 nM Cu medium by about 30% compared to the non-adapted populations. The long-term results identified one adaptive strategy of the diatom to counteract Cu limitation, but we recognize that other adaptations may emerge in other populations subjected to similar stress. As discussed below, changes in photophysiology, Cu stoichiometry and cuproenzyme expression revealed the adaptive strategy of the $LCuA_{1nM}$ population that enabled it to increase Cu use efficiency and optimize growth in a low Cu environment.

Increased fitness of low Cu-adapted cells in Cu-deficient medium

In short-term assay experiments, *T. oceanica* achieved maximum growth rate in Cu-sufficient medium (Kong and Price, 2019), ultimately limited by temperature. The increase in rate of the CCuA population (~15%) was likely a result of continuous selection for fast-growing phenotypes by the culturing method. The ancestral population used to derive the CCuA and $LCuA_{1nM}$ populations was originally maintained in batch culture and transferred approximately every two weeks when the cells reached stationary phase. In this method, cells grew exponentially when resources were initially plentiful and then entered stationary phase as a result of resource depletion. Transition from exponential to stationary growth would thus impose temporally varying selection for fast growing and survival phenotypes in the population. Transferring the CCuA and $LCuA_{1nM}$ populations prior to stationary phase eliminated selection for the survival phenotypes and enriched fast-growing phenotypes in the population. The plateauing of growth rate after 973 days (Figure 2; Supplementary Figure S1), implied that the CCuA population reached the maximum set by the environmental conditions of the experiment.

Growth rate of the $LCuA_{1nM}$ population increased dramatically during selection, by about 2-fold in relative terms (from ~0.4 to 0.8 μ_{max}). The reciprocal transplant assay showed the population grew significantly faster than the CCuA population in Cu-deficient media, but significantly slower in Cu-sufficient medium. Slower growth in Cu-sufficient medium was likely a result of a trade-off between the ability to survive at low Cu concentration and the ability for rapid growth at high Cu concentration, a typical evolutionary response. Evolutionary trade-offs mean that increased fitness in one environment may come at a cost of reduced fitness in another environment (Stearns, 1992). Trade-offs are also observed in long-term selection experiments with marine phytoplankton grown under high CO_2

TABLE 4 Gene transcript abundance of Cu-containing proteins in low Cu-adapted ($LCuA_{1nM}$) and control (CCuA) populations.

Protein name	RPKM ± 1 SD		FC	Regulation	*p*
	$LCuA_{1nM}$	CCuA		type	
Plastocyanin	5561 ± 741	3015 ± 405	1.84	up*	<0.01
Multicopper oxidase	114 ± 51	51.5 ± 12.8	2.21	up	0.11
Multicopper oxidase	14.5 ± 4.7	15.6 ± 2.5	0.93	down	0.39
Cytochrome c oxidase subunit 1	2.05 ± 0.48	2.12 ± 1.22	0.97	down	0.61
Cytochrome c oxidase subunit 2	1.04 ± 0.63	1.31 ± 0.48	0.80	down	0.46
Cytochrome c oxidase subunit 3	0.51 ± 0.14	0.97 ± 0.48	0.53	down	0.07
Cytochrome c oxidase subunit 4	654 ± 52	779 ± 120	0.83	down	0.24
Cytochrome c oxidase subunit 5b	487 ± 40	369 ± 49	1.33	up	0.23
Cytochrome c oxidase subunit 6a	531 ± 40	507 ± 107	1.05	up	0.96
Cytochrome c oxidase subunit 6b	28.3 ± 3.0	41.9 ± 6.5	0.67	down*	<0.01
Tyrosinase	0.33 ± 0.11	10.6 ± 2.3	0.03	down*	<0.0001
DBH-like monooxygenase	134 ± 115	109 ± 22	1.22	up	0.50
NADH dehydrogenase	137 ± 16	239 ± 44	0.57	down*	<0.001
NADH:ubiquinone oxidoreductase	101 ± 21	194 ± 15	0.52	down*	<0.0001

Values reported are mean RPKM (reads per kilobase of exon per million reads mapped) ± 1 standard deviation (SD). Fold-change ratios (FC) compare gene transcript abundance (RPKM values) of $LCuA_{1nM}$ and CCuA populations ($LCuA_{1nM}$/CCuA). An asterisk indicates differentially expressed genes ($p<0.01$, t-test).

and high temperature (Lohbeck et al., 2012; O'Donnell et al., 2018; Jin et al., 2022). Oceanic and coastal diatoms grow relatively faster at low and high Fe concentrations, respectively, reflecting the outcome of natural selection by the Fe concentrations of their native environments (Ryther and Kramer, 1961; Brand, 1991; Maldonado and Price, 1996). Of particular interest in the context of decreasing resource availability in the ocean is the mechanism that allowed for improved growth of the $LCuA_{1nM}$ population under Cu-limiting conditions.

Decreased cellular Cu demand

In the Cu-deficient environment, Q_{Cu} of *T. oceanica* comprised metabolic Cu contained in essential cuproenzymes, including plastocyanin, cytochrome c oxidase and multicopper oxidase (Kong and Price, 2020; Kong and Price, 2022). Storage pools were expected to be minimal under these conditions, because Cu was growth rate limiting. Lower cellular and volumetric quotas of the $LCuA_{1nM}$ compared to the CCuA and ancestral populations (Table 3) suggested adaptation reduced the cellular Cu requirement for growth. This may indeed be the case, but we note that the quotas of $LCuA_{1nM}$ cells were similar to those measured in acclimated, Cu-limited cultures by Kim and Price (2017), so they were not dramatically reduced by selection in the low Cu medium. Low quotas by themselves reveal little about the Cu requirements for growth because they need to be considered in the context of cell metabolic rate. The $LCuA_{1nM}$ cells, for example, contained 30% less Cu L^{-1} CV than the CCuA cells, but grew 1.47-fold faster. A quantitative way to evaluate the metabolic requirements is to compute the Cu use efficiency (CuCE), which expresses the rate of biomass production (mol C $cell^{-1}$ h^{-1}) per unit of limiting resource (Q_{Cu}: mol Cu $cell^{-1}$) (Raven, 1988). The calculations show that CuUE was 2.2 times higher in the $LCuA_{1nM}$ population than the CCuA population and 3.2 times higher than in the ancestral population, confirming that per unit of metabolic Cu carbon fixation rates were greatly elevated (Table 3). That faster rates of growth (and carbon assimilation) were sustained by less Cu, suggested adaptation altered cellular metabolism in the $LCuA_{1nM}$ population and reduced the demand for metabolic Cu.

Mechanism of adaptation

Physiological acclimation increases the cellular Cu uptake rate of Cu-limited cultures by more than 2-fold, enabling cells to acquire Cu more effectively at low concentrations (Hill et al., 1996; Kong and Price, 2019). Fe and Zn uptake also increase in Fe- and Zn-limited phytoplankton to compensate for reduced availability in the environment (Sunda and Huntsman, 1992; Maldonado and Price, 2001). The increase in uptake could translate into increased fitness in low metal environments compared to non-acclimated cells. Measurements of short-term uptake rate show for Fe that the maximum rate may be limited by the number of transporters physically able to fit in plasma membrane (Hudson and Morel, 1993), so that the potential for selection to increase uptake rate may be limited. Adaptation to low Cu did not increase Cu uptake capabilities of the $LCuA_{1nM}$ compared to the CCuA and ancestral populations (Table 3), but this does not rule out the possibility that other replicate populations could adapt in this way. We note in Fe-limited phytoplankton, however, that Fe uptake rate constants normalized to cell surface area are remarkably similar in taxa isolated from low and high Fe environments, suggesting low Fe availability has not selected for increased Fe uptake (Lis et al., 2015; Shaked et al., 2020).

The chlorophyll-derived physiological parameter, $rETR_{max}$, provides an estimate of the maximum photosynthetic electron transport rate and is positively correlated with growth rate in the diatom (Kim and Price, 2017). Pooled data from the $LCuA_{1nM}$, CCuA and ancestral populations showed a significant, positive relationship between growth rate and $rETR_{max}$ ($F_{(1,4)}$ = 47.1, p=0.002, Figure 4A), suggesting growth rate depended on photosynthetic electron flow and photosynthetic capacity. In *T. oceanica*, plastocyanin, the most abundant Cu-containing protein, transfers electrons from cytochrome b_6f to photosystem I (Peers and Price, 2006) and is critical to maintaining efficient photosynthetic electron flow. Its abundance decreases to about 1 µmol L^{-1} CV when Cu is limiting, but it makes up about 70% of the total Q_{Cu} under these conditions, much higher than when Cu is sufficient. Preferential retention of Cu in plastocyanin relative to other Cu-containing proteins underscores its overall importance to cellular metabolism. Kim and Price (2017) showed $rETR_{max}$ was positively correlated with Q_{Cu} in Cu-limited *T. oceanica*, consistent with the function of Cu-containing plastocyanin in photosynthesis. In the present study, $rETR_{max}$ was negatively correlated with Q_{Cu} implying that faster electron transport rates were surprisingly associated with lower cellular Cu (Figure 4B). Note that Q_{Cu} and $rETR_{max}$ data in Figure 4 were obtained from three different populations (CCuA, $LCuA_{1nM}$ and ancestral) that were adapted to different growth conditions, while Kim and Price (2017) assayed a single population under different environmental conditions. Faster rates of $rETR_{max}$ and growth were sustained by less Cu in $LCuA_{1nM}$ cells, raising the question how this diatom restored plastocyanin-dependent electron flow in the absence of additional Cu.

Rate constants of photosynthetic electron transport are positively related to the abundance of plastocyanin in cyanobacteria and green algae (Hervás et al., 1994; Hervás et al., 1995) and the efficiency of transport affected by the

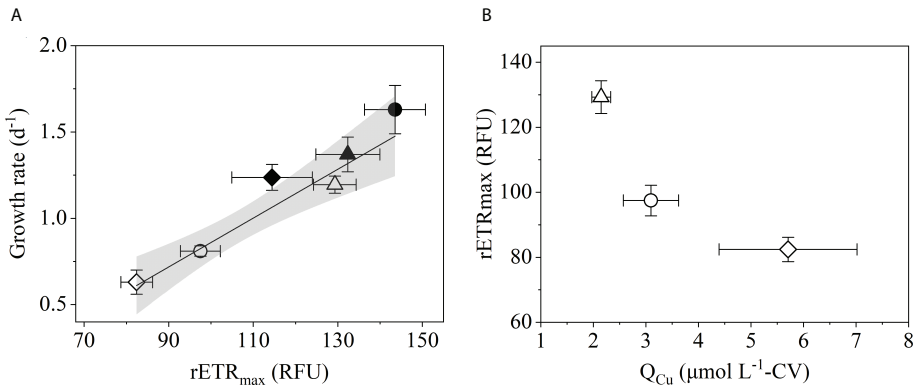

FIGURE 4
(A) Specific growth rate as a function of maximum relative electron transport rate ($rETR_{max}$) of $LCuA_{1nM}$ (◭), CCuA (◑) and ancestral (◈) populations grown in Cu-deficient (open symbols) and Cu-sufficient (filled symbols) medium. The solid line through the data points is the least squares linear regression ($F_{(1,4)}$ = 47.1, p=0.002) with the grey band indicating the 95% confidence interval. **(B)** $rETR_{max}$ as a function of Cu quota (Q_{Cu}) of $LCuA_{1nM}$ (△), CCuA (○) and ancestral (◇) *T. oceanica* populations grown in Cu-deficient medium. Error bars represent ± 1 SD of three ($rETR_{max}$ and Q_{Cu}) or ten to fifteen (growth rate) biological replicates.

structural and electrostatic properties of plastocyanin and PSI (Hippler et al., 1998; De la Rosa et al., 2002). The observation of higher plastocyanin transcript abundance in Cu-limited $LCuA_{1nM}$ cells (Table 4) was in good agreement with faster rates of electron transport compared to CCuA cells (Figure 3). Regulation of plastocyanin occurs at the protein level in *C. reinhardtii* (Merchant and Bogorad, 1986b). Plastocyanin genes are continuously transcribed in both Cu-limited and sufficient cells, but the proteins are stabilized by the presence of intracellular Cu^+ ions and rapidly degraded in their absence under Cu deficient conditions (Merchant and Bogorad, 1986b; Li and Merchant, 1995). Although the regulatory mechanisms governing the levels of plastocyanin and other cuproenzymes in *T. oceanica* are currently unknown, the unexpected increase in transcript abundance of plastocyanin and simultaneous decrease in other cuproenzymes (Table 4) imply a potential reallocation of Cu from the downregulated cuproenzymes to the plastocyanin protein. If our interpretation is correct, then it suggests that *T. oceanica* may employ a Cu-sparing pathway different from that documented in Cu-deficient *Chlamydomonas*. In *Chlamydomonas*, plastocyanin is degraded under Cu-deficiency as cytochrome c_6 replaces its function in photosynthetic electron transport (Merchant and Bogorad, 1986b). This allows Cu in plastocyanin to be preferentially allocated to other important cuproenzymes, such as cytochrome c oxidase and ferroxidase (Kropat et al., 2015). Cytochrome c_6 is present in the *T. oceanica* genome (Lommer et al., 2012), but the protein fails to restore photosynthetic competence under Cu-limiting conditions and is believed to be non-functional (Kong and Price, 2022). Thus, plastocyanin is exclusively responsible for maintaining photosynthetic electron transport in this diatom. Because of its essential and irreplaceable role, Cu demand for plastocyanin may be preferentially fulfilled at the expense of other Cu-containing catalysts. Upregulation of plastocyanin gene transcription may increase apoplastocyanin synthesis to bind additional Cu made available from the decrease/degradation in other cuproenzymes. Some uncertainty exists in this Cu-sparing strategy. For example, the regulatory mechanisms governing the expression of these cuproenzymes are unknown, so protein abundance may not be directly related to transcript abundance. The amount of reallocated Cu is also unknown, so it is difficult to estimate whether the amount is sufficient to increase plastocyanin and sustain faster rates of electron transport ($rETR_{max}$). Moreover, the reallocation of Cu, if it occurred, may cause defects in other cuproenzyme-dependent functions. Replacement isozymes with alternative cofactor dependencies may be upregulated to compensate for the loss of Cu-requiring biochemical functions. Alternatively, changes may have occurred in structural properties of PSI and its electrostatic attraction with the plastocyanin electron donor that optimized configuration of the complex and enabled a higher turnover and faster electron transport rate (De la Rosa et al., 2002; Castell et al., 2021). Biochemical and molecular studies are needed to explore these possibilities.

Data availability statement

The datasets presented in this study can be found in online repositories. The names of the repository/repositories and accession number(s) can be found in the article/Supplementary Material.

Author contributions

LK and NP designed the research; LK performed the experiments and collected raw data; LK and NP analyzed and interpreted the data; LK and NP wrote the manuscript. All authors contributed to the article and approved the submitted version.

Funding

Funding for this study was provided by the Natural Sciences and Engineering Research Council of Canada.

Acknowledgments

The authors thank Dr. Bingzhang Chen and Dr. Kailin Liu of University of Strathclyde for assistance in statistical analysis.

Conflict of interest

The authors declare that the research was conducted in the absence of any commercial or financial relationships that could be construed as a potential conflict of interest.

Publisher's note

Supplementary material

The Supplementary Material for this article can be found online at: https://www.frontiersin.org/articles/10.3389/fmars.2022.975184/full#supplementary-material

References

Avendaño, L., Gledhill, M., Achterberg, E. P., Rerolle, V., and Schlosser, C. (2016). Influence of ocean acidification on the organic complexation of iron and copper in Northwest European shelf seas; A combined observational and model study. *Front. Mar. Sci.* 3. doi: 10.3389/fmars.2016.00058

Behrenfeld, M. J., O'Malley, R. T., Siegel, D. A., McClain, C. R., Sarmiento, J. L., Feldman, G. C., et al. (2006). Climate-driven trends in contemporary ocean productivity. *Nature* 444, 752–755. doi: 10.1038/nature05317

Bertilsson, S., Berglund, O., Karl, D. M., and Chisholm, S. W. (2003). Elemental composition of marine *Prochlorococcus* and *Synechococcus*: Implications for the ecological stoichiometry of the sea. *Limnol. Oceanogr.* 48, 1721–1731. doi: 10.4319/lo.2003.48.5.1721

Boyd, P. W., and Doney, S. C. (2002). Modelling regional responses by marine pelagic ecosystems to global climate change. *Geophys. Res. Lett.* 29, 53–1-53-4. doi: 10.1029/2001GL014130

Brand, L. E. (1991). Minimum iron requirements of marine phytoplankton and the implications for the biogeochemical control of new production. *Limnol. Oceanogr.* 36, 1756–1771. doi: 10.4319/lo.1991.36.8.1756

Brand, L. E., Sunda, W. G., and Guillard, R. R. L. (1983). Limitation of marine phytoplankton reproductive rates by zinc, manganese, and iron. *Limnol. Oceanogr.* 28, 1182–1198. doi: 10.4319/lo.1983.28.6.1182

Brand, L. E., Sunda, W. G., and Guillard, R. R. L. (1986). Reduction of marine phytoplankton reproduction rates by copper and cadmium. *J. Exp. Mar. Biol. Ecol.* 96, 225–250. doi: 10.1016/0022-0981(86)90205-4

Browning, T. J., Achterberg, E. P., Rapp, I., Engel, A., Bertrand, E. M., Tagliabue, A., et al. (2017). Nutrient co-limitation at the boundary of an oceanic gyre. *Nature* 551, 242–246. doi: 10.1038/nature24063

Caldeira, K., and Wickett, M. E. (2003). Anthropogenic carbon and ocean pH. *Nature* 425, 365–365. doi: 10.1038/425365a

Castell, C., Rodríguez-Lumbreras, L. A., Hervás, M., Fernández-Recio, J., and Navarro, J. A. (2021). New insights into the evolution of the electron transfer from cytochrome f to photosystem I in the green and red branches of photosynthetic eukaryotes. *Plant Cell Physiol.* 62, 1082–1093. doi: 10.1093/pcp/pcab044

Castruita, M., Casero, D., Karpowicz, S. J., Kropat, J., Vieler, A., Hsieh, S. I., et al. (2011). Systems biology approach in *Chlamydomonas* reveals connections between copper nutrition and multiple metabolic steps. *Plant Cell* 23, 1273–1292. doi: 10.1105/tpc.111.084400

Collins, S., and Bell, G. (2004). Phenotypic consequences of 1,000 generations of selection at elevated CO_2 in a green alga. *Nature* 431, 566–569. doi: 10.1038/nature02945

De la Rosa, M. A., Navarro, J. A., Dıaz-Quintana, A., De la Cerda, B., Molina-Heredia, F. P., Balme, A., et al. (2002). An evolutionary analysis of the reaction mechanisms of photosystem I reduction by cytochrome c6 and plastocyanin. *Bioelectrochemistry* 55, 41–45. doi: 10.1016/S1567-5394(01)00136-0

Geider, R., and LaRoche, J. (2002). Redfield revisited: Variability of C: N: P in marine microalgae and its biochemical basis. *Eur. J. Phycol.* 37, 1–17. doi: 10.1017/S0967026201003456

Gledhill, M., Achterberg, E. P., Li, K., Mohamed, K. N., and Rijkenberg, M. J. A. (2015). Influence of ocean acidification on the complexation of iron and copper by organic ligands in estuarine waters. *Mar. Chem.* 177, 421–433. doi: 10.1016/j.marchem.2015.03.016

Guillard, R. R. L., and Ryther, J. H. (1962). Studies of marine planktonic diatoms: I. *Cyclotella nana* Hustedt, and *Detonula confervacea* (Cleve) Gran. *Can. J. Microbiol.* 8, 229–239. doi: 10.1139/m62-029

Hervás, M., Navarro, J. A., Diaz, A., Bottin, H., and de la Rosa, M. A. (1995). Laser-flash kinetic analysis of the fast electron transfer from plastocyanin and cytochrome c6 to photosystem I. Experimental evidence on the evolution of the reaction mechanism. *Biochemistry* 34, 11321–11326. doi: 10.1021/bi00036a004

Hervás, M., Ortega, J., Navarro, J., Miguel, A., and Bottin, H. (1994). Laser flash kinetic analysis of *Synechocystis* PCC 6803 cytochrome c6 and plastocyanin oxidation by photosystem I. *Biochim. Biophys. Acta Bioenerg.* 1184, 235–241. doi: 10.1016/0005-2728(94)90228-3

Hillebrand, H., Duselen, C.-D., Kirschtel, D., Pollingher, U., and Zohary, T. (1999). Biovolume calculation for pelagic and benthic microalgae. *J. Phycol.* 35, 403–424. doi: 10.1046/j.1529-8817.1999.3520403.x

Hill, K. L., Hassett, R., Kosman, D., and Merchant, S. (1996). Regulated copper uptake in *Chlamydomonas reinhardtii* in response to copper availability. *Plant Physiol.* 112, 697–704. doi: 10.1104/pp.112.2.697

Hippler, M., Drepper, F., Haehnel, W., and Rochaix, J.-D. (1998). The n-terminal domain of PsaF: Precise recognition site for binding and fast electron transfer from cytochrome c6 and plastocyanin to photosystem I of *Chlamydomonas reinhardtii*. *Proc. Natl. Acad. Sci. U.S.A.* 95, 7339–7344. doi: 10.1073/pnas.95.13.7339

Houghton, J. T., Ding, Y., Griggs, D. J., Noguer, M., van der Linden, P. J., Dai, X., et al. (2001). *Climate change 2001: The scientific basis* (New York: The Press Syndicate of the University of Cambridge).

Hudson, R. J. M., and Morel, F. M. M. (1993). Trace metal transport by marine microorganisms: Implications of metal coordination kinetics. *Deep Sea Res. 1 Oceanogr. Res. Pap.* 40, 129–150. doi: 10.1016/0967-0637(93)90057-A

Hutchins, D. A., Walworth, N. G., Webb, E. A., Saito, M. A., Moran, D., McIlvin, M. R., et al. (2015). Irreversibly increased nitrogen fixation in *Trichodesmium* experimentally adapted to elevated carbon dioxide. *Nat. Commun.* 6, 8155. doi: 10.1038/ncomms9155

Jacquot, J. E., Kondo, Y., Knapp, A. N., and Moffett, J. W. (2013). The speciation of copper across active gradients in nitrogen-cycle processes in the eastern tropical South Pacific. *Limnol. Oceanogr.* 58, 1387–1394. doi: 10.4319/lo.2013.58.4.1387

Jacquot, J. E., and Moffett, J. W. (2015). Copper distribution and speciation across the international GEOTRACES section GA03. *Deep Sea Res. 2 Top. Stud. Oceanogr.* 116, 187–207. doi: 10.1016/j.dsr2.2014.11.013

Jin, P., Gao, K., and Beardall, J. (2013). Evolutionary responses of a coccolithophorid *Gephyrocapsa oceanica* to ocean acidification. *Evolution* 67, 1869–1878. doi: 10.1111/evo.12112

Jin, P., Ji, Y., Huang, Q., Li, P., Pan, J., Lu, H., et al. (2022). A reduction in metabolism explains the tradeoffs associated with the long-term adaptation of phytoplankton to high CO_2 concentrations. *New Phytol.* 233, 2155–2167. doi: 10.1111/nph.17917

Joos, F., Plattner, G.-K., Stocker, T. F., Marchal, O., and Schmittner, A. (1999). Global warming and marine carbon cycle feedbacks on future atmospheric CO_2. *Science* 284, 464–467. doi: 10.1126/science.284.5413.464

Jordi, A., Basterretxea, G., Tovar-Sánchez, A., Alastuey, A., and Querol, X. (2012). Copper aerosols inhibit phytoplankton growth in the Mediterranean Sea. *Proc. Natl. Acad. Sci.* 109, 21246–21249. doi: 10.1073/pnas.1207567110

Kim, J. W., and Price, N. M. (2017). The influence of light on copper-limited growth of an oceanic diatom, *Thalassiosira oceanica* (*Coscinodiscophyceae*). *J. Phycol.* 53, 938–950. doi: 10.1111/jpy.12563

Kong, L., and Price, N. M. (2019). Functional CTR-type Cu (I) transporters in an oceanic diatom. *Environ. Microbiol.* 21, 98–110. doi: 10.1111/1462-2920.14428

Kong, L., and Price, N. M. (2020). Identification of copper-regulated proteins in an oceanic diatom, *Thalassiosira oceanica* 1005. *Metallomics* 12, 1106–1117. doi: 10.1039/d0mt00033g

Kong, L., and Price, N. M. (2022). Transcriptomes of an oceanic diatom reveal the initial and final stages of acclimation to copper deficiency. *Environ. Microbiol.* 24, 951–966. doi: 10.1111/1462-2920.15609

Kropat, J., Gallaher, S. D., Urzica, E. I., Nakamoto, S. S., Strenkert, D., Tottey, S., et al. (2015). Copper economy in *Chlamydomonas*: Prioritized allocation and reallocation of copper to respiration vs. photosynthesis. *Proc. Natl. Acad. Sci. U.S.A.* 112, 2644–2651. doi: 10.1073/pnas.1422492112

LaRoche, J., Boyd, P. W., McKay, R. M. L., and Geider, R. J. (1996). Flavodoxin as an *in situ* marker for iron stress in phytoplankton. *Nature* 382, 802–805. doi: 10.1038/382802a0

Li, H., and Merchant, S. S. (1995). Degradation of plastocyanin in copper-deficient *Chlamydomonas reinhardtii*. evidence for a protease-susceptible conformation of the apoprotein and regulated proteolysis. *J. Biol. Chem.* 270, 23504–23510. doi: 10.1074/jbc.270.40.23504

Lis, H., Shaked, Y., Kranzler, C., Keren, N., and Morel, F. M. M. (2015). Iron bioavailability to phytoplankton: An empirical approach. *ISME J.* 9, 1003–1013. doi: 10.1038/ismej.2014.199

Litchman, E., Edwards, K. F., Klausmeier, C. A., and Thomas, M. K. (2012). Phytoplankton niches, traits and eco-evolutionary responses to global environmental change. *Mar. Ecol. Prog. Ser.* 470, 235–248. doi: 10.3354/meps09912

Lohbeck, K. T., Riebesell, U., and Reusch, T. B. (2012). Adaptive evolution of a key phytoplankton species to ocean acidification. *Nat. Geosci.* 5, 346–351. doi: 10.1038/ngeo1441

Lommer, M., Specht, M., Roy, A.-S., Kraemer, L., Andreson, R., Gutowska, M. A., et al. (2012). Genome and low-iron response of an oceanic diatom adapted to chronic iron limitation. *Genome Biol.* 13, R66. doi: 10.1186/gb-2012-13-7-r66

Maldonado, M. T., and Price, N. M. (1996). Influence of N substrate on Fe requirements of marine centric diatoms. *Mar. Ecol. Prog. Ser.* 141, 161–172. doi: 10.3354/meps141161

Maldonado, M. T., and Price, N. M. (2001). Reduction and transport of organically bound iron by *Thalassiosira oceanica* (*Bacillariophyceae*). *J. Phycol.* 37, 298–310. doi: 10.1046/j.1529-8817.2001.037002298.x

McDonnell, C. S. (2015). *Adaptive response of a marine Chlamydomonas sp. to phosphorus limitation* ([Montreal (QC)]: McGill University).

Merchant, S. S., Allen, M. D., Kropat, J., Moseley, J. L., Long, J. C., Tottey, S., et al. (2006). Between a rock and a hard place: Trace element nutrition in *Chlamydomonas*. *Biochim. Biophys. Acta Mol. Cell. Res.* 1763, 578–594. doi: 10.1016/j.bbamcr.2006.04.007

Merchant, S. S., and Bogorad, L. (1986a). Regulation by copper of the expression of plastocyanin and cytochrome c552 in *Chlamydomonas reinhardi*. *Mol. Cell. Biol.* 6, 462–469. doi: 10.1128/MCB.6.2.462

Merchant, S. S., and Bogorad, L. (1986b). Rapid degradation of apoplastocyanin in Cu(II)-deficient cells of *Chlamydomonas reinhardtii*. *J. Biol. Chem.* 261, 15850–15853. doi: 10.1016/S0021-9258(18)66641-4

Merchant, S. S., and Helmann, J. D. (2012). Elemental economy: microbial strategies for optimizing growth in the face of nutrient limitation. *Adv. Microb. Physiol.* 60, 91–210. doi: 10.1016/B978-0-12-398264-3.00002-4

Merilä, J., and Hendry, A. P. (2014). Climate change, adaptation, and phenotypic plasticity: the problem and the evidence. *Evol. Appl.* 7, 1–14. doi: 10.1111/eva.12137

Millero, F. J., Woosley, R., Ditrolio, B., and Waters, J. (2009). Effect of ocean acidification on the speciation of metals in seawater. *Oceanography* 22, 72–85. doi: 10.5670/oceanog.2009.98

Mills, M. M., Ridame, C., Davey, M., LaRoche, J., and Geider, R. J. (2004). Iron and phosphorus co-limit nitrogen fixation in the eastern tropical north Atlantic. *Nature* 429, 292–294. doi: 10.1038/nature02550

Moffett, J. W., and Dupont, C. (2007). Cu complexation by organic ligands in the sub-arctic NW Pacific and Bering Sea. *Deep Sea Res. 1 Oceanogr. Res. Pap.* 54, 586–595. doi: 10.1016/j.dsr.2006.12.013

Moore, C. M., Mills, M. M., Arrigo, K. R., Berman-Frank, I., Bopp, L., Boyd, P. W., et al. (2013). Processes and patterns of oceanic nutrient limitation. *Nat. Geosci.* 6, 701–710. doi: 10.1038/ngeo1765

Morel, F. M. M. (1987). Kinetics of nutrient uptake and growth in phytoplankton. *J. Phycol.* 23, 137–150. doi: 10.1111/j.1529-8817.1987.tb04436.x

O'Donnell, D. R., Hamman, C. R., Johnson, E. C., Kremer, C. T., Klausmeier, C. A., and Litchman, E. (2018). Rapid thermal adaptation in a marine diatom reveals constraints and trade-offs. *Glob. Change Biol.* 24, 4554–4565. doi: 10.1111/gcb.14360

Orr, J. C. (2011). "Recent and future changes in ocean carbonate chemistry," in *Ocean acidification*. Eds. J.-P. Gattuso and L. Hansson (New York: Oxford), 41–66.

Page, M. D., Kropat, J., Hamel, P. P., and Merchant, S. S. (2009). Two *Chlamydomonas* CTR copper transporters with a novel cys-met motif are localized to the plasma membrane and function in copper assimilation. *Plant Cell* 21, 928–943. doi: 10.1105/tpc.108.064907

Paytan, A., Mackey, K. R., Chen, Y., Lima, I. D., Doney, S. C., Mahowald, N., et al. (2009). Toxicity of atmospheric aerosols on marine phytoplankton. *Proc. Natl. Acad. Sci.* 106, 4601–4605. doi: 10.1073/pnas.0811486106

Peers, G., and Price, N. M. (2006). Copper-containing plastocyanin used for electron transport by an oceanic diatom. *Nature* 441, 341–344. doi: 10.1038/nature04630

Peers, G., Quesnel, S.-A., and Price, N. M. (2005). Copper requirements for iron acquisition and growth of coastal and oceanic diatoms. *Limnol. Oceanogr.* 50, 1149–1158. doi: 10.4319/lo.2005.50.4.1149

Price, N. M., Harrison, G. I., Hering, J. G., Hudson, R. J., Nirel, P. M. V., Palenik, B., et al. (1989). Preparation and chemistry of artificial algal culture medium Aquil. *Biol. Oceanogr.* 6, 443–461. doi: 10.1080/01965581.1988.10749544

Ralph, P. J., and Gademann, R. (2005). Rapid light curves: a powerful tool to assess photosynthetic activity. *Aquat. Bot.* 82, 222–237. doi: 10.1016/j.aquabot.2005.02.006

Raven, J. A. (1988). The iron and molybdenum use efficiencies of plant growth with different energy, carbon and nitrogen sources. *New Phytol.* 109, 279–287. doi: 10.1111/j.1469-8137.1988.tb04196.x

R Core Team (2020). *R: A language and environment for statistical computing* (Vienna, Austria: R Foundation for Statistical Computing). Available at: https://www.R-project.org/.

Ryther, J. H., and Kramer, D. D. (1961). Relative iron requirement of some coastal and offshore plankton algae. *Ecology* 42, 444–446. doi: 10.2307/1932105

Sarmiento, J. L., Hughes, T. M., Stouffer, R. J., and Manabe, S. (1998). Simulated response of the ocean carbon cycle to anthropogenic climate warming. *Nature* 393, 245–249. doi: 10.1038/30455

Schaum, C., Buckling, A., Smirnoff, N., Studholme, D. J., and Yvon-Durocher, G. (2018). Environmental fluctuations accelerate molecular evolution of thermal tolerance in a marine diatom. *Nat. Commun.* 9, 1–14. doi: 10.1038/s41467-018-03906-5

Schlüter, L., Lohbeck, K. T., Gröger, J. P., Riebesell, U., and Reusch, T. B. (2016). Long-term dynamics of adaptive evolution in a globally important phytoplankton species to ocean acidification. *Sci. Adv.* 2, e1501660. doi: 10.1126/sciadv.1501660

Schlüter, L., Lohbeck, K. T., Gutowska, M. A., Gröger, J. P., Riebesell, U., and Reusch, T. B. (2014). Adaptation of a globally important coccolithophore to ocean

warming and acidification. *Nat. Clim. Change* 4, 1024–1030. doi: 10.1038/nclimate2379

Semeniuk, D. M., Bundy, R. M., Payne, C. D., Barbeau, K. A., and Maldonado, M. T. (2015). Acquisition of organically complexed copper by marine phytoplankton and bacteria in the northeast subarctic Pacific Ocean. *Mar. Chem.* 173, 222–233. doi: 10.1016/j.marchem.2015.01.005

Shaked, Y., Buck, K. N., Mellett, T., and Maldonado, M. T. (2020). Insights into the bioavailability of oceanic dissolved Fe from phytoplankton uptake kinetics. *ISME J.* 14, 1182–1193. doi: 10.1038/s41396-020-0597-3

Stearns, S. C. (1992). The evolution of life histories. *Oxford: Oxford Univ. Press*.

Strzepek, R. F., and Harrison, P. J. (2004). Photosynthetic architecture differs in coastal and oceanic diatoms. *Nature* 431, 689–692. doi: 10.1038/nature02954

Strzepek, R. F., Hunter, K. A., Frew, R. D., Harrison, P. J., and Boyd, P. W. (2012). Iron-light interactions differ in Southern Ocean phytoplankton. *Limnol. Oceanogr.* 57, 1182–1200. doi: 10.4319/lo.2012.57.4.1182

Strzepek, R. F., and Price, N. M. (2000). Influence of irradiance and temperature on the iron content of the marine diatom *Thalassiosira weissflogii* (*Bacillariophyceae*). *Mar. Ecol. Prog. Ser.* 206, 107–117. doi: 10.3354/meps206107

Sunda, W. G., and Guillard, R. R. L. (1976). The relationship between cupric ion activity and the toxicity of copper to phytoplankton. *J. Mar. Res.* 34, 511–529. Available at: www.journalofmarineresearch.org

Sunda, W. G., and Huntsman, S. A. (1992). Feedback interactions between zinc and phytoplankton in seawater. *Limnol. Oceanogr.* 37, 25–40. doi: 10.4319/lo.1992.37.1.0025

Sunda, W. G., and Huntsman, S. A. (1995). Regulation of copper concentration in the oceanic nutricline by phytoplankton uptake and regeneration cycles. *Limnol. Oceanogr.* 40, 132–137. doi: 10.4319/lo.1995.40.1.0132

Sunda, W. G., Swift, D. G., and Huntsman, S. A. (1991). Low iron requirement for growth in oceanic phytoplankton. *Nature* 351, 55–57. doi: 10.1038/351055a0

Takeda, S., Obata, H., Okubo, A., Sato, M., and Kondo, Y. (2014)."Bioavailability and biogeochemical processes of trace metals in the surface ocean," in *Western Pacific air-Sea interaction study*. Eds. M. Uematsu, Y. Yokouchi, Y. W. Watanabe, S. Takeda and Y. Yamanaka (Tokyo: TERRAPUB), 163–176.

Taylor, G. T., Muller-Karger, F. E., Thunell, R. C., Scranton, M. I., Astor, Y., Varela, R., et al. (2012). Ecosystem responses in the southern Caribbean Sea to global climate change. *Proc. Natl. Acad. Sci. U.S.A.* 109, 19315–19320. doi: 10.1073/pnas.1207514109

Tong, S., Gao, K., and Hutchins, D. A. (2018). Adaptive evolution in the coccolithophore *Gephyrocapsa oceanica* following 1,000 generations of selection under elevated CO_2. *Glob. Change Biol.* 24, 3055–3064. doi: 10.1111/gcb.14065

Whitby, H., Posacka, A. M., Maldonado, M. T., and van den Berg, C. M. G. (2018). Copper-binding ligands in the NE Pacific. *Mar. Chem.* 204, 36–48. doi: 10.1016/j.marchem.2018.05.008

Zhang, J., Xu, H., Lan, J., Ai, L., Sheng, E., Yan, D., et al. (2020). Weakening dust storm intensity in arid central Asia due to global warming over the past 160 years. *Front. Earth Sci.* 8, 284. doi: 10.3389/feart.2020.00284

Zong, Q., Mao, R., Gong, D. Y., Wu, C., Pu, B., Feng, X., et al. (2021). Changes in dust activity in spring over East Asia under a global warming scenario. *Asia Pac. J. Atmos. Sci.* 57, 839–850. doi: 10.1007/s13143-021-00224-7